Potential of Mean Force Calculations of the Stacking–Unstacking Process in Single-Stranded Deoxyribodinucleoside Monophosphates

Jan Norberg and Lennart Nilsson
Center for Structural Biology, Department of Biosciences at NOVUM, Karolinska Institute, S-141 57 Huddinge, Sweden

ABSTRACT The free energy of the stacking–unstacking process of deoxyribodinucleoside monophosphates in aqueous solution has been investigated by potential of mean force calculations along a reaction coordinate, defined by the distance between the glycosidic nitrogen atoms of the bases. The stacking–unstacking process of a ribodinucleoside monophosphate was observed to be well characterized by this coordinate, which has the advantage that it allows for a dynamical backbone and flexible bases. All 16 naturally occurring DNA dimers composed of the adenine, cytosine, guanine, or thymine bases in both the 5′ and the 3′ positions were studied. From the free-energy profiles we observed the deepest minima for the stacked states of the purine–purine dimers, but good stacking was also observed for the purine–pyrimidine and pyrimidine–purine dimers. Substantial stacking ability was found for the dimers composed of a thymine base and a purine base and also for the deoxythymidylyl-3′,5′-deoxythymidine dimer. Very poor stacking was observed for the dCpdC dimer. Conformational properties and solvent accessibility are discussed for the stacked and unstacked dimers. The potential of mean force profiles of the stacking–unstacking process for the DNA dimers are compared with the RNA dimers.

INTRODUCTION

The three-dimensional structure of DNA is stabilized by, e.g., base stacking, hydrogen bonding, electrostatic interactions, and solvent effects. In contrast to the hydrogen bonding responsible for base pairing, base stacking interactions are critically dependent on the aromatic base sequence in the single or double helix. Base stacking has been studied in a number of different nucleic acids, ranging from nucleotides to polynucleotides. The smallest DNA system in which sequence-dependent effects can be studied is a deoxyribodinucleoside monophosphate. A number of extensive experimental studies have revealed important information about the conformational properties and dynamics of ribodinucleoside monophosphates in aqueous solution (Frechet et al., 1979, and references therein), but only a few have focused on deoxyribodinucleoside monophosphates. For example, conformational characteristics of the naturally occurring deoxyribodinucleoside monophosphates have been investigated by nuclear magnetic resonance spectroscopy (Cheng and Sarma, 1977). Theoretical studies on dimers usually focus on the base–base interactions and leave out the dynamical backbone and/or the influence of solvent effects. Potential energy calculations have been used to investigate minimum energy conformations of deoxyribodinucleoside monophosphates (Broyde et al., 1975, 1978; Thiyagarajan and Ponnusway, 1978). An ab initio molecular orbital study (Aida, 1988) evaluated the inter- and intrastrand stacking interaction energy in B-DNA. The free-energy contributions to the base stacking have been analyzed with the finite-difference Poisson–Boltzmann method to treat the electrostatic interactions between bases only in aqueous solution (Friedman and Honig, 1995). We have performed molecular dynamics simulations on the ribodinucleoside monophosphate guanylyl-3′,5′-uridine in aqueous solution to study conformational changes and solvent effects (Norberg and Nilsson, 1994a,b). An earlier potential of mean force calculation studied the stacking of the 9-methyladenine and 1-methylthymine bases in solution but without the backbone (Dang and Kollman, 1990). Potential of mean force (PMF) calculations (Norberg and Nilsson, 1995a) have been used to study the temperature dependence of the stacking propensity of an RNA dimer, adenylyl-3′,5′-adenosine, with results in agreement with experimental data. The free-energy profiles of going from a stacked conformation to an unstacked were also investigated previously for all the naturally occurring ribodinucleoside monophosphates (Norberg and Nilsson, 1995b). The 2′OH group in the RNA riboses and the 5-methyl group in the DNA thymine bases must, because they are the only chemical differences between RNA and DNA, determine the conformational properties of these molecules and hence also the differences in stability of DNA and RNA helices (Saenger, 1988; Wang and Kool, 1995).

Received for publication 11 July 1995 and in final form 25 August 1995.

Address reprint requests to Dr. Lennart Nilsson, Center for Structural Biology, Department of Biosciences at NOVUM, S141 57 Huddinge, Sweden. Tel.: +46-8-608-9228; Fax: +46-8-608-9290; E-mail: lennart.nilsson@csb.ki.se.

Abbreviations used: dApdA, deoxyadenylyl-3′,5′-deoxyadenosine; dApdC, deoxyadenylyl-3′,5′-deoxycytidine; dApdG, deoxyadenylyl-3′,5′-deoxyguanosine; dApdT, deoxyadenylyl-3′,5′-deoxythymidine; dCpdA, deoxycytidylyl-3′,5′-deoxyadenosine; dCpdC, deoxycytidylyl-3′,5′-deoxycytidine; dCpdG, deoxycytidylyl-3′,5′-deoxyguanosine; dCpdT, deoxycytidylyl-3′,5′-deoxythymidine; dGpdA, deoxyguanylyl-3′,5′-deoxyadenosine; dGpdC, deoxyguanylyl-3′,5′-deoxycytidine; dGpdG, deoxyguanylyl-3′,5′-deoxyguanosine; dGpdT, deoxyguanylyl-3′,5′-deoxythymidine; dTpdA, deoxythymidylyl-3′,5′-deoxyadenosine; dTpdC, deoxythymidylyl-3′,5′-deoxycytidine; dTpdG, deoxythymidylyl-3′,5′-deoxyguanosine; dTpdT, deoxythymidylyl-3′,5′-deoxythymidine; dUpdU, deoxyuridylyl-3′, 5′-deoxyuridine; MD, molecular dynamics; PMF, potential of mean force; ASA, accessible surface area.

0006-3495/95/12/2277/09 $2.00

Here we report the potential of mean force calculations of all the 16 naturally occurring deoxyribodinucleoside monophosphates fully solvated in water to examine the transition between stacked and unstacked states, in both thermodynamic and structural terms. The PMF profiles were generated from molecular dynamics simulations, allowing us to extract detailed information about conformational changes.

MATERIALS AND METHODS

The initial conformation of each deoxyribodinucleoside monophosphate was generated from x-ray fiber diffraction data (Arnott et al., 1976) as a single-stranded stacked standard B-DNA. The initial distance between the glycosidic nitrogen atoms in the DNA dimers was 4.417 Å. A sodium counterion was placed on the bisector of the phosphate oxygens to produce an electrically neutral system. Each of the deoxyribodinucleoside monophosphates was energy minimized 100 cycles of steepest descent. Energy minimizations and simulations were performed with the CHARMM program (Brooks et al., 1983) with the all-atom parameters (MacKerell et al., in press). Each of the deoxyribodinucleoside monophosphates was immersed in a 25.0-Å side cubic box of TIP3P water molecules (Jorgensen et al., 1983). Water molecules that overlapped the solute were deleted, and the remaining water molecules were energy minimized 100 cycles of steepest descent and 3000 cycles of adopted-basis set Newton-Raphson (Brooks et al., 1983), while the solute was constrained with a harmonic potential with a force constant of 1.0 kcal·mol^{-1}·Å^{-2}. Periodic boundary conditions were applied to handle the surface effects. The hydrogen atom–heavy atom bond lengths were constrained by the SHAKE algorithm (Ryckaert et al., 1977) to make a time step of 2 fs possible in the integration of the equations of motion, which were carried out with the Verlet algorithm (Verlet, 1967). A relative dielectric constant of 1.0 was used, and the nonbonded interactions were smoothly shifted to zero at a cutoff of 11.5 Å (Brooks et al., 1983). The atom-based nonbonded list was updated every 20 steps, and the coordinates were saved every 20 steps. Initial velocities for the simulations were assigned according to a Maxwell–Boltzmann distribution corresponding to 300 K, and the temperature was periodically checked and kept within a window of ±5K from 300 K. All the molecular dynamics simulations were performed on DEC AXP 3000/400 workstations.

Potential of mean force

The potential of mean force $w(R)$ (Beveridge and DiCapua, 1989; Straatsma and McCammon, 1992), i.e., the free-energy content, is a function of the reaction coordinate R, and the Helmholtz free energy takes the form

$$w(R) = -k_B T \ln \rho^*(R) - E_{restr}(R)$$

where k_B is the Boltzmann constant, T is the temperature, and $\rho^*(R)$ is the probability distribution, in the presence of the restraining umbrella potential $E_{restr}(R)$, which is applied because it is difficult to obtain adequate sampling along R in only one unrestrained simulation. For the umbrella sampling along the reaction coordinate we used a harmonic restraining potential

$$E_{restr}(R) = k(R_{NxNy} - R_{ref})^2$$

where k is the force constant and R_{NxNy} is the distance, which in each simulation window will be restrained to the reference value R_{ref}. As the reaction coordinate we chose the distance between the glycosidic nitrogen atoms of the bases (Nx, Ny = $N1$ for pyrimidine and $N9$ for purine) (Fig. 1). The PMF pieces from the different simulation windows were processed and spliced together by use of an extension of the weighted-histogram analysis method (Boczko and Brooks, 1993; Kumar et al., 1992).

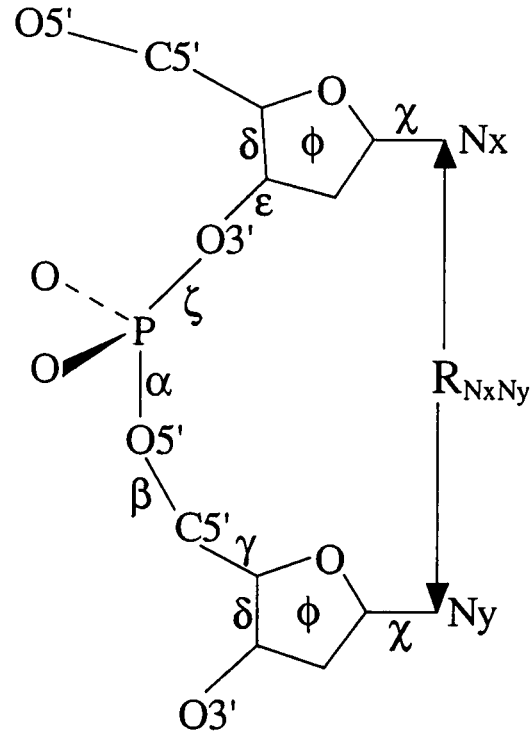

FIGURE 1 Definition of the reaction coordinate, which connects the base glycosidic nitrogen atoms, used in the PMF calculations and of the backbone and glycosidic torsion angles and pseudorotation phase angles.

Simulations

Each of the systems, the aqueous solvated dimer and the counterion, was first equilibrated for a period of 40 ps. During this equilibration period the restrained distance was set to 4.5 Å with a force constant of 4.0 kcal·mol^{-1}·Å^{-2}. Thereafter the conformational space was sampled by performing MD simulations in 18 windows with R_{ref} varying from 3.5 to 12.0 Å in 0.5-Å intervals. The force constant was set to 16.0 kcal·mol^{-1}·Å^{-2} such that neighboring sampling windows overlapped. In each window the simulation was started from a snapshot of the preceding window, and, after 5 ps of equilibration, conformations were sampled for 20–100 ps. The longer simulation times were required in the R_{ref} = 5- to 10-Å range, where the dimer has left the stacked state and the bases become more flexible. In an unrestrained MD simulation of an unstacked ribodinucleoside monophosphate the majority of conformations were obtained in the 6- to 9-Å range (Norberg and Nilsson, 1994a). The total simulation time for all 16 deoxyribodinucleoside monophosphates was 14.2 ns.

RESULTS

Base–base interactions

To evaluate the importance of direct base–base interactions for stacking, the interaction energy between the aromatic bases for stacked and unstacked conformations was determined. The base–base interaction energy difference between stacked and unstacked states was calculated by

$$\Delta E_{b-b} = \langle E_{b-b} \rangle_{4.5} - \langle E_{b-b} \rangle_{9.0}$$

where $\langle \cdots \rangle_i$ denotes the time average of the interaction energy over the trajectory obtained in the MD simulation with the distance R_{NxNy} restrained to 4.5 Å (i = 4.5) and 9.0

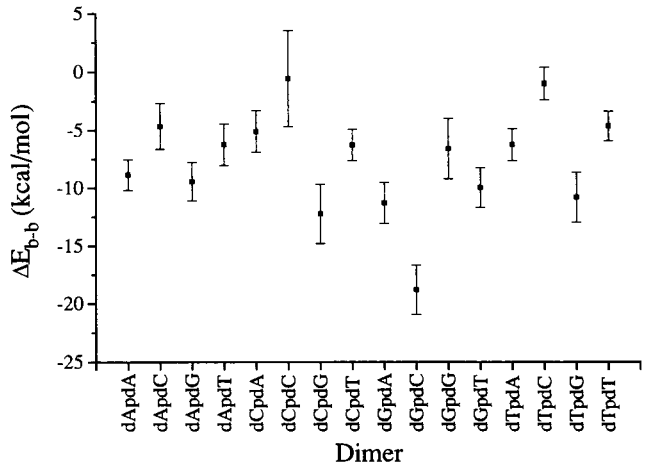

FIGURE 2 Base–base interaction energy differences ΔE_{b-b} between stacked (R_{NxNy} = 4.5 Å) and unstacked (R_{NxNy} = 9.0 Å) DNA dimers. The error bars displayed are the largest standard deviation of the energy for the stacked or the unstacked form.

Å (i = 9.0), corresponding to stacked and unstacked states, respectively.

The base–base interaction energy most favorable for stacking was obtained for the dGpdC dimer, which also has been seen in ab initio calculations of just B-DNA base–base interactions (Aida, 1988). Low base–base interaction energy differences were also observed for dApdA and dCpdG and for dimers containing combinations of a guanine base and either an adenine base or a thymine base (Fig. 2).

The least favorable base–base interactions were obtained for the cytosine-containing dimers dTpdC and dCpdC, which also had very large root mean square fluctuations of the base–base interaction energy. All the dimers except the dCpdC dimer showed root mean square fluctuations of 1.3–2.6 kcal/mol.

PMF profiles

The equilibrium between stacked and unstacked states is determined by their free-energy difference, i.e., their PMFs,

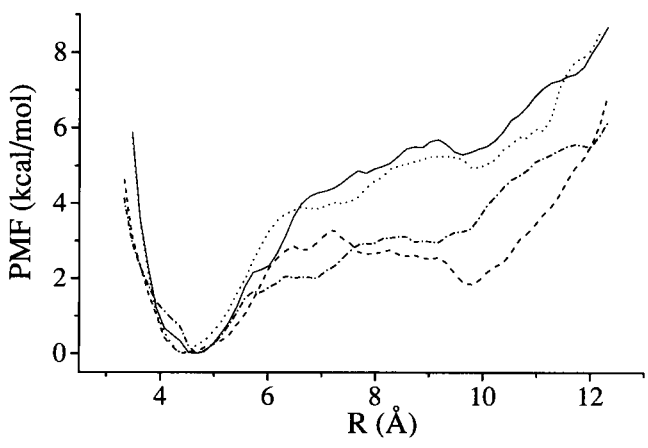

FIGURE 3 PMF profiles of the deoxyribodinucleoside monophosphates dApdA (——), dApdC (- - - -), dApdG (-·-·-) and dApdT (·····).

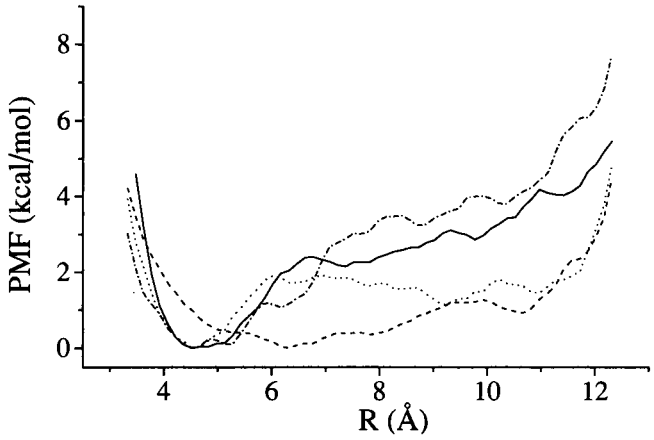

FIGURE 4 PMF profiles of the deoxyribodinucleoside monophosphates dCpdA (——), dCpdC (- - - -), dCpdG (-·-·-) and dCpdT (·····).

as displayed in Figs. 3-6. The PMF is at a 4- to 6-kcal/mol higher level for the unstacked states of the dApdA and dApdT dimers than for the stacked state where the PMFs have a minimum, but for the dApdC and dApdG dimers most of the unstacked states are only 2–3 kcal/mol higher (Fig. 3).

The unstacked states of the dCpdA and dCpdG dimers were 2–4 kcal/mol higher than the stacked states, and for the dCpdT dimer the difference was 1–2 kcal/mol (Fig. 4). No major differences were found between the shapes of the PMF profiles of the dApdC and dCpdA dimers. For the dCpdC dimer we did not observe any significant increase in free energy for the unstacked states. The relatively large flexibility of the bases in the dCpdC dimer was also found from the large fluctuations of the base–base interaction energy (Fig. 2).

The unstacked states for the dGpdA dimer were 4.5–6.5 kcal/mol higher than the stacked states (Fig. 5), 1–2 kcal/mol higher than for the dApdG dimer. Although the base–base interaction energy would indicate that the dGpdC

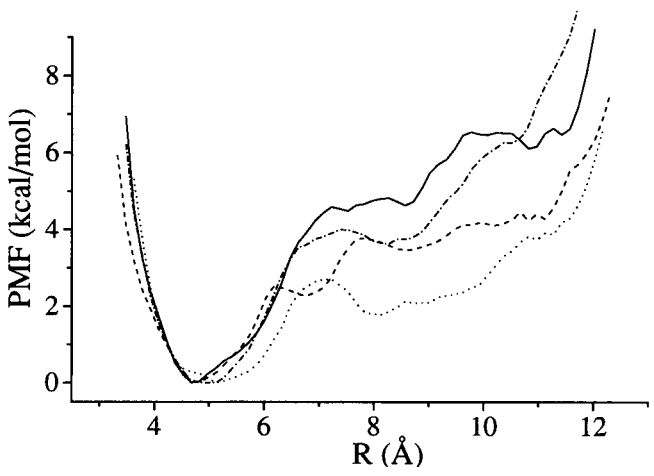

FIGURE 5 PMF profiles of the deoxyribodinucleoside monophosphates dGpdA (——), dGpdC (- - - -), dGpdG (-·-·-) and dGpdT (·····).

dimer (Fig. 2) stacks best, the PMF for dGpdC showed only a 2.5-kcal/mol deep minimum for the stacked state. The shapes of the PMF profiles for the dGpdC (Fig. 5) and dCpdG (Fig. 4) dimers were also very similar. For the dGpdG dimer we found the unstacked states more than 3.5 kcal/mol above the stacked minimum, and the dGpdT dimer preferred stacking with approximately 2 kcal/mol.

A rather broad minimum was observed for the dTpdA dimer, which still had the unstacked states approximately 4 kcal/mol higher than the stacked. The dApdT dimer (Fig. 3) showed a minimum that was narrower than but equally deep as the dTpdA dimer (Fig. 6). For the dTpdC dimer, which had poor base–base interactions (Fig. 2), the unstacked states were 1–2 kcal/mol higher than the stacked state, as also was seen for the dCpdT dimer (Fig. 4). The dTpdG dimer (Fig. 6) and the dGpdT dimer (Fig. 5) also had very similar PMF profiles, with 2-kcal/mol higher unstacked states than stacked. The pyrimidine–pyrimidine dimer dTpdT showed rather good stacking, with unstacked states 2–5 kcal/mol higher than the stacked.

For the dimers with a well-pronounced minimum near 4.5–4.7 Å, the minimum corresponded rather well to the stacked x-ray fiber diffraction structure (Arnott et al., 1976), where the distance between the glycosidic nitrogen atoms was 4.417 Å. Purine-containing dimers, especially those that contained an adenine base, showed the best stacking ability overall. Among the pyrimidine–pyrimidine dimers the best stacking ability was found for the dTpdT dimer.

In a free-energy perturbation calculation, using just the bases, Cieplak and Kollman (1988) found stacking preferences in water ordered as G/C > A/A > A/T, albeit with less than 0.5-kcal/mol difference between the G/C and A/T cases, in contrast to experimental data (Nakano and Igarahsi, 1970) indicating the order A/A > A/T > G/C. Of these three combinations we found dGpdC to stack less well than dApdA or dApdT. The differences are small, and the limited sampling leads to uncertainties that make features in the PMFs of a magnitude smaller than approximately 0.5 kcal/mol insignificant, but the dGpdC PMF (Fig. 5) levels off at a decidedly lower level than does dApdA (Fig. 3). There are several possible explanations for the difference between our present results and those of Cieplak and Kollman (1988), besides the use of two different potential energy functions for the solute. The direct base–base interactions favor G/C (Fig. 2), so there must be other driving forces involving the solvent or the backbone, or both, that lower the stacking tendency of dGpdC.

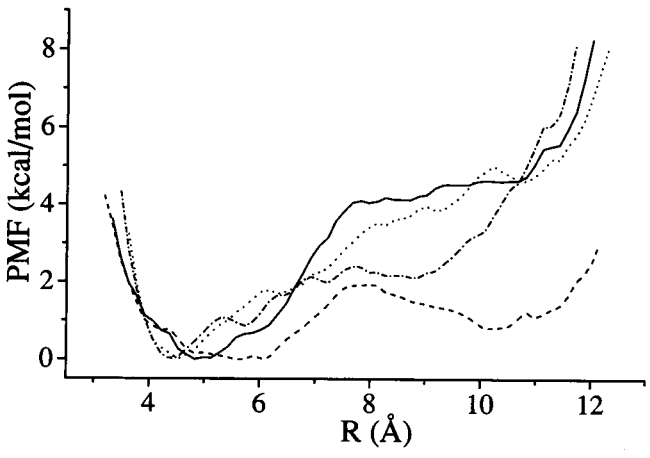

FIGURE 6 PMF profiles of the deoxyribodinucleoside monophosphates dTpdA (——), dTpdC (- - - -), dTpdG (-·-·-) and dTpdT (····).

Conformational changes

To show the unfolding pathway of the dApdA dimer, snapshots from the simulations at the restrained distances to 4.5, 5.5, 6.5, 7.5, 8.5, 9.5, 10.5, and 11.5 Å are displayed in Fig. 7.

The dynamical behavior of the backbone and glycosidic torsion angles and pseudorotation phase angles was analyzed with the program Dials and Windows (Ravishanker et al., 1989) and is displayed for the dApdA, dApdT, dTpdA, and dTpdT dimers at the restrained distances to 4.5, 7.0, 9.0, and 11.0 Å (Figs. 8, 9, 10, and 11). The time evolution of the angles is shown by dials with 0° at the top and angles increasing in the clockwise direction and with $t = 0$ ps at the center of the circle. The δ torsion angles were fluctuating between the initial B-DNA conformation and a value near 79° corresponding to an A-DNA conformation (Saenger, 1988). Most of the ϵ angles became more positive compared with those in the initial conformation. A shift of approximately -90° of the ζ angle was observed for the dApdA dimer restrained to 7.0, 9.0, and 11.0 Å for the dApdT dimer restrained to 11.0 Å and for the dTpdT dimer restrained to 11.0 Å. A slightly more negative α angle was obtained for shorter restrained distances. The β angle

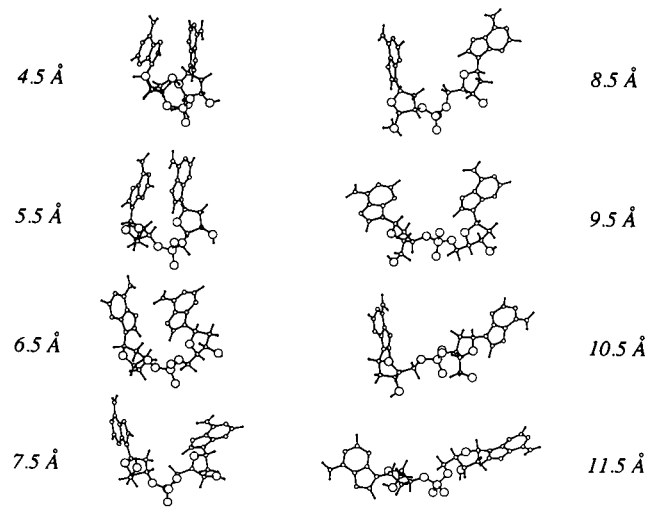

FIGURE 7 Snapshots from the MD simulations of the dApdA dimer at the restrained distances to 4.5, 5.5, 6.5, 7.5, 8.5, 9.5, 10.5, and 11.5 Å. The structures were generated with Quanta (Molecular Simulation, Inc., Burlington, MA).

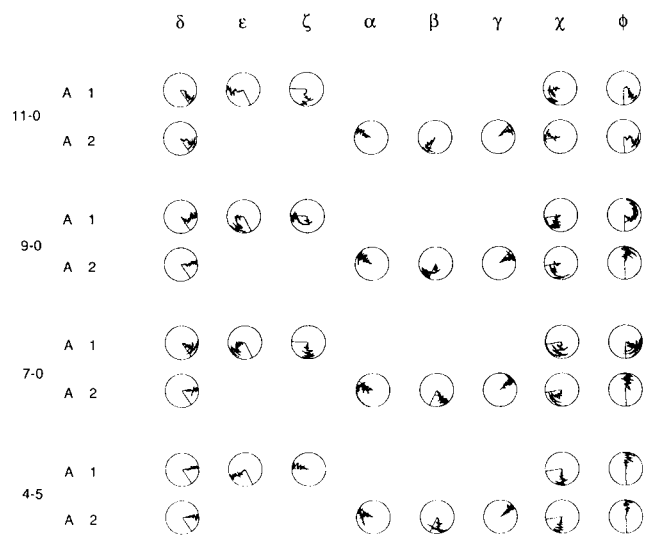

FIGURE 8 Backbone and glycosidic torsion angles and pseudorotation phase angles of the dApdA dimer for the distances restrained at 4.5, 7.0, 9.0, and 11.0 Å. The 5′ base is indicated by 1 and the 3′ base by 2.

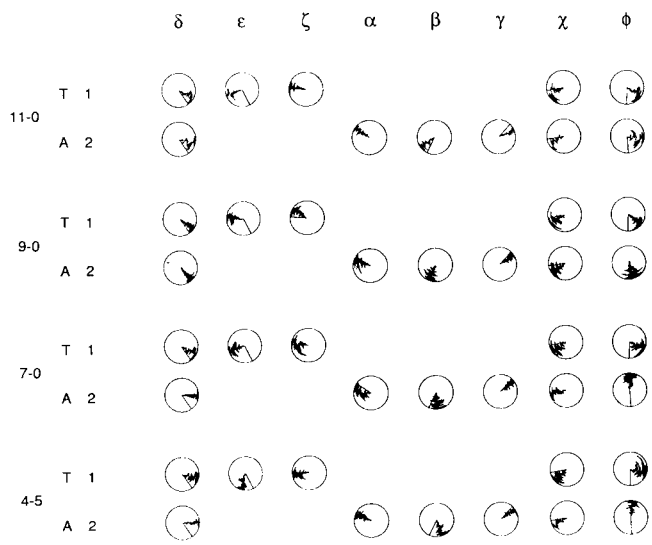

FIGURE 10 Backbone and glycosidic torsion angles and pseudorotation phase angles of the dTpdA dimer for the distances restrained at 4.5, 7.0, 9.0, and 11.0 Å. The 5′ base is indicated by 1 and the 3′ base by 2.

was observed to go from a more negative value at shorter restrained distances to a value less negative at a distance restrained to 11.0 Å, passing through the initial value at the distance restrained to 9.0 Å. The γ angle was observed to be close to the initial value and slightly more positive at longer restrained distances. For the χ angles we found changes between the initial value of the χ angle and near the value of the A-DNA conformation, -158° (Saenger, 1988). The pseudorotation phase angles changed mainly from the C2′-endo mode to the C3′-endo mode. The C1′-exo and the O4′-endo modes were occupied mainly at the distances restrained to 11.0 Å. At the distance restrained to 4.5 Å we found a preference for the C3′-endo mode for the sugar moieties connected to a adenine base in the dimers; overall the conformation of the dimers in the stacked state was more similar to A-DNA than to B-DNA.

Accessible surface area

Inasmuch as stacking is known to be favored in water more than in organic solvents (Cantor and Schimmel, 1980; Saenger, 1988), we calculated the solvent accessible surface area (Lee and Richard, 1971) for every simulation along the reaction coordinate (Figs. 12 and 13). A spherical probe radius of 1.4 Å, corresponding to the average radius of a water molecule (Alden and Kim, 1979), was used to deter-

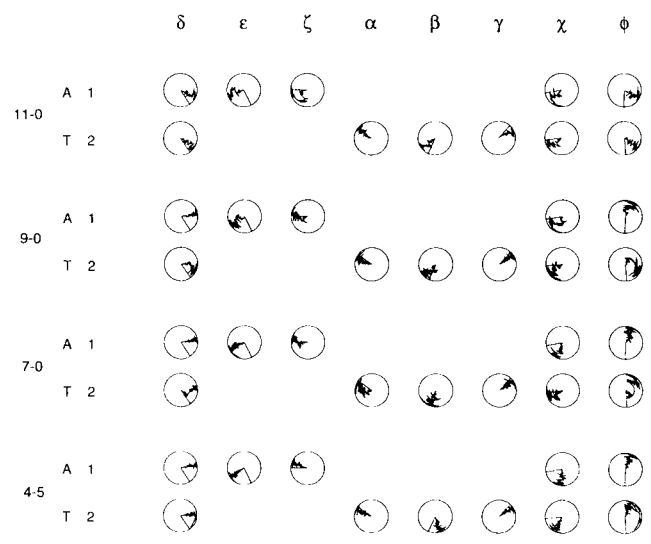

FIGURE 9 Backbone and glycosidic torsion angles and pseudorotation phase angles of the dApdT dimer for the distances restrained at 4.5, 7.0, 9.0, and 11.0 Å. The 5′ base is indicated by 1 and the 3′ base by 2.

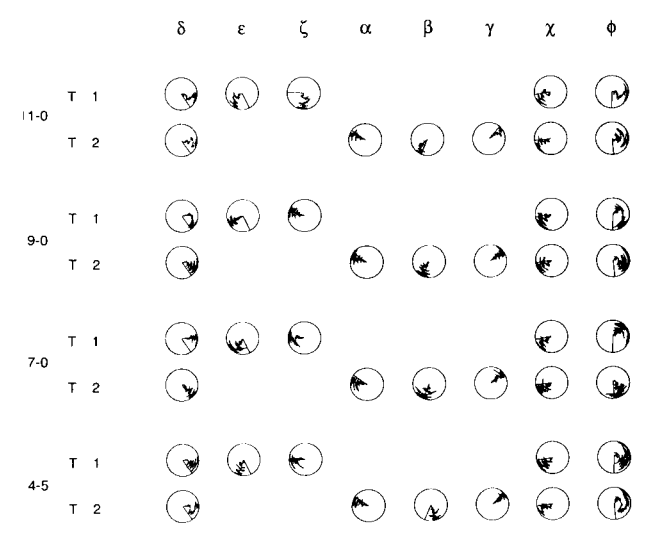

FIGURE 11 Backbone and glycosidic torsion angles and pseudorotation phase angles of the dTpdT dimer for the distances restrained at 4.5, 7.0, 9.0, and 11.0 Å. The 5′ base is indicated by 1 and the 3′ base by 2.

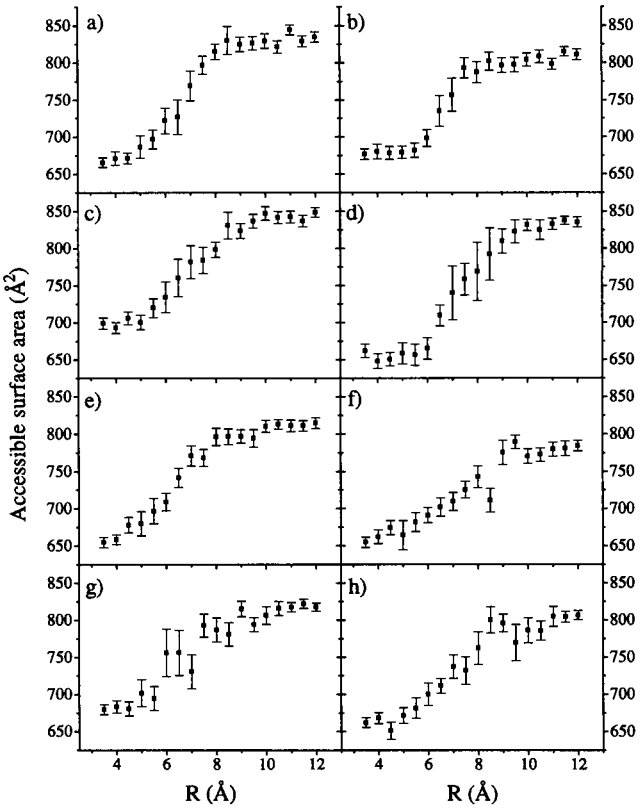

FIGURE 12 The accessible surface area versus restrained distance of *a*) dApdA, *b*) dApdC, *c*) dApdG, *d*) dApdT, *e*) dCpdA, *f*) dCpdC, *g*) dCpdG, and *h*) dCpdT. The error bars indicate the standard deviations.

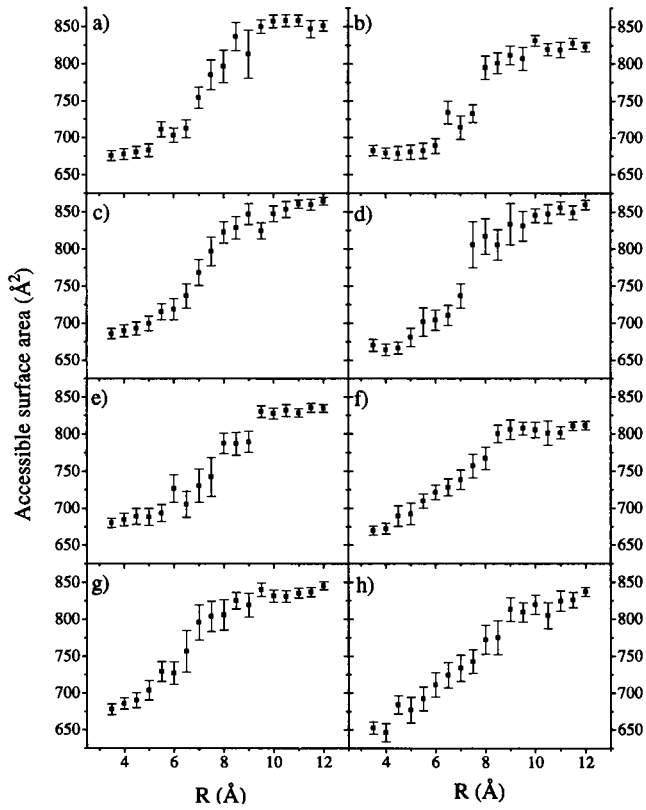

FIGURE 13 The accessible surface area versus restrained distance of *a*) dGpdA, *b*) dGpdC, *c*) dGpdG, *d*) dGpdT, *e*) dTpdA, *f*) dTpdC, *g*) dTpdG, and *h*) dTpdT. The error bars indicate the standard deviations.

mine the ASA. For the dimers with a high stacking propensity (mainly purine-containing dimers) we found a sigmoidal shape of the ASA as a function of R_{NxNy}, with no major changes for $R_{NxNy} < 6.0$ Å. Instead the ASA changed in the interval 6.0–9.0 Å, and thereafter the ASA remained rather constant because the bases were fully exposed. For the dimers showing poor stacking ability, a more gradual, almost linear, increase of the ASA was obtained starting from distances restrained to ~5 Å. The largest standard deviations of the ASA were observed in the 6- to 9-Å range of the restrained distances, where the major conformational changes of the dimers occurred, going from a stacked state to an unstacked.

The dimers with largest and smallest ASA were the guanine- and cytosine-containing dimers, respectively. This can also be seen from the ASA of the individual bases as presented in Table 1, which also shows a breakdown of the ASA in polar and nonpolar components for the deoxyribose, the ribose, the phosphate group, and the base moities of DNA and RNA.

Hydrophobic forces are of major importance for many molecular processes, including protein folding (Ha et al., 1989; Livingstone et al, 1991), for which their contribution toward stabilizing the folded conformation has been found to be directly proportional to the nonpolar surface area buried on folding (Livingstone et al., 1991). We can see from Table 1 that the deoxyribose sugar has the largest nonpolar ASA, the guanine base the smallest (except for the totally polar phosphate group) nonpolar ASA, and the thymine base the largest nonpolar ASA of the bases, equal in size to the ribose sugar, with the other bases between guanine and thymine. The ASA, and its polar and nonpolar components, was calculated for the stacked and unstacked conformations of the 16 DNA dimers (Table 2) and for purposes of comparison also for a dUpdU dimer obtained by

TABLE 1 Accessible surface area (Å²) of nucleic acid components

Structure	Total area	Polar area	Nonpolar area
Ribose*	313	177	136
Deoxyribose*	300	95	205
PO_2‡	184	184	0
Adenine§	294	202	92
Cytosine§	268	182	86
Guanine§	306	248	58
Thymine§	297	164	133
Uracil§	257	171	86

*The hydrogen atoms of the 5′ and 3′ terminals were not included in the ribose and deoxyribose.

‡In this group only the phosphorous atom and the two oxygens atoms not involved in the ester bonds have been included.

§The base only.

TABLE 2 Accessible surface area (Å²) of dimers sorted by increasing ΔA_{np} = nonpolar surface area difference between stacked and unstacked conformations

Structure	Stacked conformation*			Unstacked conformation‡				
	Total§	Polar†	Nonpolar¶	Total§	Polar†	Nonpolar¶	ΔA_p**	ΔA_{np}‡‡
dTpdC	692	362	330	804	441	363	79	33
dCpdC	676	387	289	774	448	326	61	37
dGpdG	717	461	256	860	564	296	103	40
dGpdA	674	398	276	837	519	318	121	42
dApdA	676	354	322	851	478	373	124	51
dGpdC	667	398	269	834	513	321	115	52
"dUpdU"§§	662	379	283	776	432	344	53	61
dCpdG	671	411	260	819	498	321	87	61
dTpdA	687	373	314	834	455	379	82	65
dCpdT	661	357	304	772	402	370	45	66
dApdC	672	390	282	785	434	351	44	69
dCpdA	672	391	281	814	463	351	72	70
dApdG	696	421	275	855	508	347	87	72
dTpdG	696	414	282	826	472	354	58	72
dGpdT	665	402	263	855	512	343	110	80
dTpdT	692	356	336	831	409	422	53	86
dApdT	661	367	294	824	435	389	68	95

*Final conformation of 4.5-Å window simulation.
‡Final conformation of 11.0-Å window simulation.
§Total solvent accessible surface area calculated using the Lee–Richards (1971) algorithm with a probe radius of 1.4 Å.
†Solvent accessible surface area of polar atoms (O, N, P, and their covalently bound hydrogens).
¶Solvent accessible surface are of nonpolar atoms (C and hydrogens covalently attached to carbon atoms).
**Solvent accessible surface area difference between unstacked and stacked conformations for polar atoms.
‡‡Solvent accessible surface area difference between unstacked and stacked conformations for non-polar atoms.
§§Obtained from the dTpdT structures by replacing the 5-methyl of the thymines with hydrogens.

replacement of the 5-methyls in dTpdT with hydrogens. The values given in Table 2 are from single structures, and, from the error bars given at R_{NxNy} = 4.5 and 11.0 Å in Figs. 12 and 13, would be accurate to within ±5–10 Å².

The large nonpolar ASA of thymine is also evident in the thymine-containing dimers. The hydrophobic free energy, ΔG_{hyd}, driving protein folding, e.g., is roughly proportional to ΔA_{np}, the nonpolar surface area buried on folding, with a proportionality constant of ~22 cal·mol^{-1}·Å^{-2} at 300 K (Ha et al., 1989). Assuming that the same relation also holds for the nucleic acid fragments in this study, the data in Table 2 suggest that ΔG_{hyd} for stacking of these dimers range from ~0.7 kcal/mol for dTpdC to ~2 kcal/mol for dApdT. It is obvious that the 5-methyl in thymine provides a substantial nonpolar area to be protected from solvent; the ~12 Å²/methyl as indicated by the comparison between dTpdT and dUpdU in Table 2 would provide ~0.25 kcal/mol for shielding of each methyl from solvent.

It is also clear that the stacking propensities shown by the PMFs (Figs. 3–6) are not directly correlated with the ΔA_{np} data in Table 2, even though some dimers with low (dTpdC, dCpdC) or high (dApdT) stacking tendencies have a correspondingly small or large ΔA_{np}.

Comparison between DNA and RNA dimers

The conformations of the DNA dimers in the stacked state (simulations with R_{NxNy} restrained to 4.5 Å) were very similar to those of the corresponding RNA dimers (Norberg and Nilsson, 1995b), clearly of an A-DNA/A-RNA type, even though the initial setup was in the B-DNA conformation for the DNA dimers and in the A-RNA conformation for the RNA dimers. Because short oligonucleotides are frequently found to be of the A-type (Saenger, 1988) this is not very surprising. It could possibly be an effect of the potential energy function used or a result of the distance restraint. The potential energy function (MacKerell et al., in press) in CHARMM contains the correction term for deoxyriboses (Olson, 1982; Olson and Sussman, 1982), and we also found tendencies for the A-type in a 60-ps MD simulation of the dApdA dimer without any restraint (data not shown); hence we do not think that these effects are very large. Consequently the direct base–base interaction energies were also very similar. Also, in a comparison of thymine in the DNA case with uracil in the RNA case, the 5-methyl in thymine does not provide stacking stabilization through van der Waals interactions with the other base.

The differences in stacking between DNA and RNA must be due to the 2′-hydroxyl in RNA or to the 5-methyl in the thymines of DNA, and in a recent thermal denaturation study Wang and Kool (1995) found that the 5-methyl always stabilizes various helical RNA and DNA complexes, whereas the 2′-hydroxyl could be either stabilizing or destabilizing. Free-energy perturbation calculations (Plaxco and Goddard, 1994) estimate that shielding of the 5-methyl from solvent provides approximately 1 kcal/mol in stabilizing free energy. A comparison of stacking stabilities as indicated by the DNA PMFs (Figs. 3–6) with the corre-

sponding RNA PMFs (Norberg and Nilsson, in press) yields a similar picture. Of the seven dimers containing thymine, five had PMFs with a more well-developed minimum at the stacked conformation than the corresponding PMFs with uracil, and one (dTpdG) was similar for DNA and RNA. Only the dGpdT dimer stacked less well than its RNA counterpart. Of the nine remaining cases, in which the only difference is the 2′-hydroxyl, three are similar, three stack better in the DNA form (dApdC, dCpdG, dGpdG), and three are less stably stacked than in the RNA form (dApdG, dCpdA, dGpdC).

In the DNA dimers we did not see such large differences in stacking between dimers with reversed order of the bases as were found for RNA, where, e.g., CpA stacked considerably better than ApC or GpC better than CpG; both ApU and dApdT did, however, stack better than UpA and dTpdA, respectively.

CONCLUSIONS

PMF calculations have been used to explore the free energy of the stacking–unstacking process of deoxyribodinucleoside monophosphates in aqueous solution. The strongest base–base interactions were found for the dGpdC dimer. We found the stacking propensity of the dimers to be very sequence dependent, which should be important in the stabilization of a B-DNA double helix. Dimers containing at least one purine base showed good stacking, with the unstacked states $\geq$2 kcal/mol higher in free energy than the stacked.

Comparing DNA with RNA showed that the 5-methyl of thymine enhanced stacking, whereas the 2′-hydroxyl could have either stabilizing or destabilizing effects, in agreement with recent data on RNA and DNA helical stability (Wang and Kool, 1995). Good stacking was found for the dTpdT dimer, but the RNA UpU dimer exhibits no stacking at all (Norberg and Nilsson, 1995b). The lowest stacking ability was obtained for the dCpdC dimer.

The structural expansion occurring during the unstacking process, as forced by the umbrella potential applied in the PMF calculations, was manifested mainly in the ζ-backbone torsion angles, accompanied by changes also in other backbone torsion angles and by some sugar repuckering.

For the dimers that stacked well we found a sigmoidal change of the solvent accessible surface area in the 6.0- 9.0-Å range of the distance R_{NxNy} between the glycosidic nitrogens of the bases. When $R_{NxNy} > 9.0$ Å the dimers were nearly totally exposed to water. A quite linear change of the accessible surface area was found for the dimers that did not stack so well, because the bases became flexible at shorter distances, $R_{NxNy} < 6.0$ Å.

Neither the direct interactions between the bases nor the hydrophobic free energy gained by removing nonpolar surface from water on stacking correlated directly with the stacking ability, in accord with measurements (Newcomb and Gellman, 1994), showing that stacking is the result of a delicate balance between sometimes opposing forces.

REFERENCES

Aida, M. 1988. An ab initio molecular orbital study on the sequence-dependency of DNA conformation: an evaluation of intra- and inter-strand stacking interaction energy. *J. Theor. Biol.* 130:327–335.

Alden, C. J., and S.-H. Kim. 1979. Solvent-accessible surfaces of nucleic acids. *J. Mol. Biol.* 132:411–434.

Arnott, S., P. J. C. Smith, and R. Chandrasekaran. 1976. Atomic coordinates and molecular conformations for DNA-DNA, RNA-RNA, and DNA-RNA helices. *In* CRC Handbook of Biochemistry and Molecular Biology: Nucleic Acids, 3rd ed., Vol. 2. G. D. Fasman, editor. CRC Press, Cleveland, OH. 411–422.

Beveridge, D. L., and F. M. DiCapua. 1989. Free energy via molecular simulation: applications to chemical and biomolecular systems. *Annu. Rev. Biophys. Biophys. Chem.* 18:431–492.

Boczko, E. M., and C. L. Brooks III. 1993. Constant-temperature free energy surfaces for physical and chemical processes. *J. Phys. Chem.* 97:4509–4513.

Brooks, B. R., R. E. Bruccoleri, B. D. Olafson, D. J. States, S. Swaminathan, and M. Karplus. 1983. CHARMM: a program for macromolecular energy, minimization, and dynamics calculations. *J. Comp. Chem.* 4:187–217.

Broyde, S. B., S. D. Stellman, and R. M. Wartell. 1975. The A and B conformations of DNA and RNA subunits. Potential energy calculations for dGpdC. *Biopolymers.* 14:2625–2637.

Broyde, S., R. M. Wartell, S. D. Stellman, and B. Hingerty. 1978. Minimum energy conformations of DNA dimeric subunits: potential energy calculations for dGpdC, dApdA, dCpdC, dGpdG, and dTpdT. *Biopolymers.* 17:1485–1506.

Cantor, R. C., and P. R. Schimmel. 1980. Biophysical Chemistry. Freeman, San Francisco, CA.

Cheng, D. M., and R. H. Sarma. 1977. Intimate details of the conformational characteristics of deoxyribodinucleoside monophosphates in aqueous solution. *J. Am. Chem. Soc.* 99:7333–7348.

Cieplak, P., and P. A. Kollman. 1988. Calculation of the free energy of association of nucleic acid bases in vacuo and water solution. *J. Am. Chem. Soc.* 110:3734–3739.

Dang, L. X., and P. A. Kollman. 1990. Molecular dynamics simulations study of the free energy of association of 9-methyladenine and 1-methylthymine bases in water. *J. Am. Chem. Soc.* 112:503–507.

Frechet, D., R. Ehrlich, P. Remy, and J. Gabarro-Arpa. 1979. Thermal pertubation differential spectra of ribonucleic acids. II. Nearest neighbour interactions. *Nucleic Acids Res.* 7:1981–2001.

Friedman, R. A., and B. Honig. 1995. Free energy analysis of nucleic acid base stacking in aqueous solution. *Biophys. J.* 69:1528–1535.

Ha, J.-H., R. S. Spolar, and T. M. Record, Jr. 1989. Role of the hydrophobic effect in stability of site-specific protein-DNA complexes. *J. Mol. Biol.* 209:801–816.

Jorgensen, W. L., J. Chandrasekhar, J. D. Madura, R. W. Impey, and M. L. Klein. 1983. Comparison of simple potential functions for simulating liquid water. *J. Chem. Phys.* 79:926–935.

Kumar, S., D. Bouzida, R. H. Swendsen, P. A. Kollman, and J. M. Rosenberg. 1992. The weighted histogram analysis method for free-energy calculations on biomolecules. I. The method. *J. Comp. Chem.* 13:1011–1021.

Lee, B., and F. M. Richards. 1971. The interpretation of protein structures: estimation of static accessibility. *J. Mol. Biol.* 55:379–400.

Livingstone, J. R., R. S. Spolar, and M. T. Record. 1991. Contribution to the thermodynamics of protein folding from the reduction in water-accessible nonpolar surface area. *Biochemistry.* 30:4237–4244.

MacKerell, A. D., Jr., J. Wiórkiewicz-Kuczera, and M. Karplus. 1995. An all-atom empirical energy function for the simulation of nucleic acids. *J. Am. Chem. Soc.* (in press).

Nakano, N. I., and S. J. Igarashi. 1970. Molecular interactions of pyrimidines, purines, and some other heteroaromatic compounds in aqueous media. *Biochemistry.* 9:577–583.

Newcomb, L. F., and S. H. Gellman. 1994. Aromatic stacking interactions in aqueous solution: evidence that neither classical hydrophobic effects nor dispersion forces are important. *J. Am. Chem. Soc.* 116:4993–4994.

Norberg, J., and L. Nilsson. 1994a. Stacking-unstacking of the dinucleoside monophosphate guanylyl-3′,5′-uridine studied with molecular dynamics. *Biophys. J.* 67:812–824.

Norberg, J., and L. Nilsson. 1994b. High-pressure molecular dynamics of a nucleic acid fragment. *Chem. Phys. Lett.* 224:219–224.

Norberg, J., and L. Nilsson 1995a. Temperature dependence of the stacking propensity of the adenylyl-3′,5′-adenosine. *J. Phys. Chem.* 99: 13056–13058.

Norberg, J., and L. Nilsson. 1995b. Stacking free energy profiles for all 16 natural ribodinucleoside monophosphates in aqueous solution. *J. Am. Chem. Soc.* In press.

Olson, W. K. 1982. How flexible is the furanose ring? 2. An updated potential energy estimate. *J. Am. Chem. Soc.* 104:278–286.

Olson, W. K., and J. L. Sussman. 1982. How flexible is the furanose ring? 1. A comparison of experimental and theoretical studies. *J. Am. Chem. Soc.* 104:270–278.

Plaxco, K. W., and W. A. Goddard III. 1994. Contributions of the thymine methyl group to the specific recognition of poly- and mononucleotides: an analysis of the relative free energies of solvation of thymine and uracil. *Biochemistry.* 33:3050–3054.

Ravishanker, G., S. Swaminathan, D. L. Beveridge, R. Lavery, and H. Sklenar. 1989. Conformational and helicoidal analysis of 30 ps of molecular dynamics on the d(CGCGAATTCGCG) double helix: "curves, dials and windows." *J. Biomol. Struct. Dyn.* 6:669–699.

Ryckaert, J.-P., G. Ciccotti, and H. J. C. Berendsen. 1977. Numerical integration of the Cartesian equations of motion of a system with constraints: molecular dynamcis of n-alkanes. *J. Comput. Phys.* 23: 327–341.

Saenger, W. 1988. Principles of Nucleic Acid Structure. Springer-Verlag, New York.

Straatsma, T. P., and J. A. McCammon. 1992. Computational alchemy. *Annu. Rev. Phys. Chem.* 43:407–435.

Thiyagarajan, P., and P. K. Ponnuswamy. 1978. Conformational characteristics of dApdA, dApdT, dTpdA, and dTpdT from energy minimization studies. *Biopolymers.* 17:533–553.

Verlet, L. 1967. Computer "experiments" on classical fluids. I. Thermodynamical properties of Lennards-Jones molecules. *Phys. Rev.* 159:98–103.

Wang, S., and E. T. Kool. 1995. Origins of the large differences in stability of DNA and RNA helices: C-5 methyl and 2′-hydroxyl effects. *Biochemistry.* 34:4125–4132.